Europace (2015) **17**, 326–333
doi:10.1093/europace/euu122

BASIC SCIENCE

Effects of L-type calcium channel and human ether-a-go-go related gene blockers on the electrical activity of the human heart: a simulation study

Nejib Zemzemi[1]* and Blanca Rodriguez[2]

[1]Carmen team, INRIA Bordeaux Sud-Ouest, 200 avenue de la vieille tour, Talence Cedex 33405, France; and [2]Department of Computer Science, University of Oxford, Oxford OX1 3QD, UK

Received 9 October 2013; accepted after revision 11 April 2014; online publish-ahead-of-print 16 September 2014

Aims Class III and IV drugs affect cardiac human ether-a-go-go related gene (I_{Kr}) and L-type calcium (I_{CaL}) channels, resulting in complex alterations in repolarization with both anti- and pro-arrhythmic consequences. Interpretation of their effects on cellular and electrocardiogram (ECG)-based biomarkers for risk stratification is challenging. As pharmaceutical compounds often exhibit multiple ion channel effects, our goal is to investigate the simultaneous effect of I_{CaL} and I_{Kr} block on human ventricular electrophysiology from ionic to ECG level.

Methods and results Simulations are conducted using a human body torso bidomain model, which includes realistic representation of human membrane kinetics, anatomy, and fibre orientation. A simple block pore model is incorporated to simulate drug-induced I_{CaL} and I_{Kr} blocks, for drug dose = 0, IC_{50}, 2× IC_{50}, 10× IC_{50}, and 30× IC_{50}. Drug effects on human ventricular activity are quantified for different degrees and combinations of I_{CaL} and I_{Kr} blocks from the ionic to the body surface ECG level. Electrocardiogram simulations show that I_{CaL} block results in shortening of the QT interval, ST elevation, and reduced T-wave amplitude, caused by reduction in action potential duration and action potential amplitude during the plateau phase, and in repolarization times. In contrast, I_{Kr} block results in QT prolongation and reduced T-wave amplitude. When I_{CaL} and I_{Kr} blocks are combined, the degree of I_{CaL} block strongly determines QT interval whereas the effect of I_{Kr} block is more pronounced on the T-wave amplitude.

Conclusion Our simulation study provides new insights into the combined effect of I_{CaL} and I_{Kr} blocks on human ventricular activity using a multiscale computational human torso model.

Keywords hERG block • L-type calcium block • QT interval • ECG modelling • Computer simulation • Dispersion of repolarization

Introduction

Calcium (Ca^{2+}) is the ionic link in cardiac excitation–contraction coupling, which, in cardiac cells, starts following the upstroke of the action potential (AP) and causes the opening of the L-type voltage-dependent Ca^{2+} channels. These ion channels are expressed by the CACNA1C gene. L-type Ca^{2+} channels constitute one of the most important Ca^{2+} entry pathways into the cell and have been classified by their sensitivity to dihydropyridine-based compounds (e.g. nifedipine). Different compounds have been developed to target calcium channels and in particular L-type calcium channels. The compounds aim to modulate the cardiac ventricular L-type Ca^{2+} current (I_{CaL}). These agents have been classified to three main classes: phenylalkylamines (e.g. verapamil), benzothiazepines (e.g. diltiazem), and dihydropyridines (e.g. nifedipine).[1] Calcium channel blockers have wide clinical applicability and they are used to decrease blood pressure in patients with hypertension. Calcium channel blockers are also frequently used to alter heart

* Corresponding author. Tel: +33 5 24 57 41 80. *E-mail address*: nejib.zemzemi@inria.fr

What's new?

- A mathematical model of the human cardiac ventricles embedded in a torso is used to simulate the effect of multiple ion channel block on the electrical activity of the heart from ion channel to electrocardiogram.
- L-type calcium block results in QT interval shortening, ST elevation, and T-wave amplitude reduction, caused by decrease in action potential duration and action potential amplitude and in dispersion of repolarization.
- When L-type calcium current (I_{CaL}) and rapidly activating potassium current (I_{Kr}) blocks are simultaneously applied, QT interval is more sensitive to the degree of I_{CaL} block whereas T-wave amplitude is mostly determined by I_{Kr} block.

rate, to prevent cerebral vasospasm, and to reduce chest pain caused by angina pectoris. However, it has been shown that they could increase the mortality rate in elderly patients, and have been known to have multiple side effects.[2,3] They have also been associated with a risk of cancer.[4] Abnormalities in I_{CaL}, in particular, have also been linked to ventricular arrhythmias, impaired excitation–contraction coupling leading to heart failure, as well as atrial fibrillation.[5] These abnormalities could be related to cardiac diseases or to drug-induced side effects. In both cases, they result in ionic currents abnormalities, which cause alterations in both ventricular depolarization and repolarization properties.

Of particular concern are changes in ventricular repolarization caused by combined I_{CaL} and rapidly activating potassium current (I_{Kr}) alterations, which can manifest themselves as changes in the QT interval and T-wave of the electrocardiogram (ECG), and have been linked to increased risk of arrhythmic death. QT prolongation is considered an indicator of increased risk of torsades de pointes and can lead to the abandonment of the compound development. However, some QT prolonging drugs present no arrhythmic episodes and some others are known to be useful antiarrhythmic drugs for most patients. Interpretation of drug-induced effects on the ECG is however challenging due to the variability of cardiac substrates and also to the frequent multichannel action of most compounds.[6–9] Therefore, a better understanding of drug-induced changes in the ECG and how they relate to ionic mechanisms and arrhythmic risk is needed.

Recent reviews have highlighted how computational modelling and simulation can help in the investigation of arrhythmias and antiarrhythmic therapy.[10–13] Recent studies have specifically shown the usefulness of whole-ventricular computer simulations to investigate drug effects on the electrical activity of the heart.[9,14–16] In this study, we aim at using a multiscale computational human torso model to investigate and quantify the combined effect of I_{CaL} and I_{Kr} block on human ventricular activity from the ionic to the ECG level.

Methods

Human multiscale torso–heart model

A human model of the cardiac ventricles embedded in a torso is used and illustrated in *Figure 1A* and *B*. The human ventricular model includes realistic representation of human ventricular kinetics, anatomy, and fibre orientation as previously described in Zemzemi *et al.*[15] Briefly, the anatomical model is based on data presented in Chapelle *et al.*[17] and the computational mesh contains 2 401 151 vertices and 14 336 528 tetrahedral elements.[15] The Ten Tusscher and Panfilov human AP model[18] is used to represent human membrane kinetics throughout the myocardium, including epicardial, endocardial, and mid-myocardial ionic properties based on transmural location. Therefore, transmural heterogeneity in the human AP was introduced in our human ventricular model, in agreement with previous studies such as Okada *et al.*[19]

The human ventricular model is coupled to the diffusion equation in the torso to take into account the propagation of the electrical wave from heart to torso to compute the ECGs on the body surface.[15,20]

To simulate sinus rhythm activation, a time-dependent stimulus of 0.5 ms duration and 100 mA cm^{-3} strength is applied to the endocardium. To mimic Purkinje network activation, the endocardium surface is then progressively activated from apex to base to produce a simulated activation sequence illustrated in *Figure 1A*, in line with the experimental results by Durrer *et al.*[21]

Drug/ion channel interaction model

The human AP model[18] was modified to enable simulation of drug action on I_{CaL} and I_{Kr} using the simple pore block model[7,15,22]. The degree of channel block is a function of drug concentration and the drug half maximal inhibitory concentration (IC_{50}) value for the targeted ionic channel. Thus, for a given drug dose [D] and IC_{50} value with respect to the channel j the formulation of drug action on the ionic current conductance g_j is given by:

$$g_j([D]) = g_j\left(\frac{1}{1+\left(\frac{[D]}{IC_{50}}\right)^n}\right)$$

with Hill coefficient $n = 1$.

Computational methods and data analysis

All the simulations in this paper have been conducted using the software CHASTE (Cancer Heart and Soft Tissue Environment).[23,24] Details of models and numerical methods are as described in the supplementary material in Zemzemi *et al.*[15] Simulations were run in the Bordeaux federative platform for research in computer sciences and mathematics called PLAFRIM (https://plafrim.bordeaux.inria.fr/).

We compute the standard 12-lead ECG by extracting the electrical potential values at the standard 9 electrode locations on the body surface of the human torso model.[15] A snapshot of the distribution of the electrical potential on the body surface from which the ECG is obtained is represented in *Figure 1B*. In the results of this study, all the ECG-based biomarkers are quantified for the second Einthoven lead of the ECG. The QT interval is computed as the time interval between the Q- and the T-wave peak of the ECG. At each ventricular node, the the action potential duration at 90% (APD_{90}) is computed as the time interval between the depolarization time and the time at which the transmembrane potential is 90% repolarized. Electrophysiological alterations caused by ionic current block are also described by analysing APD_{90} and AP morphology in one selected

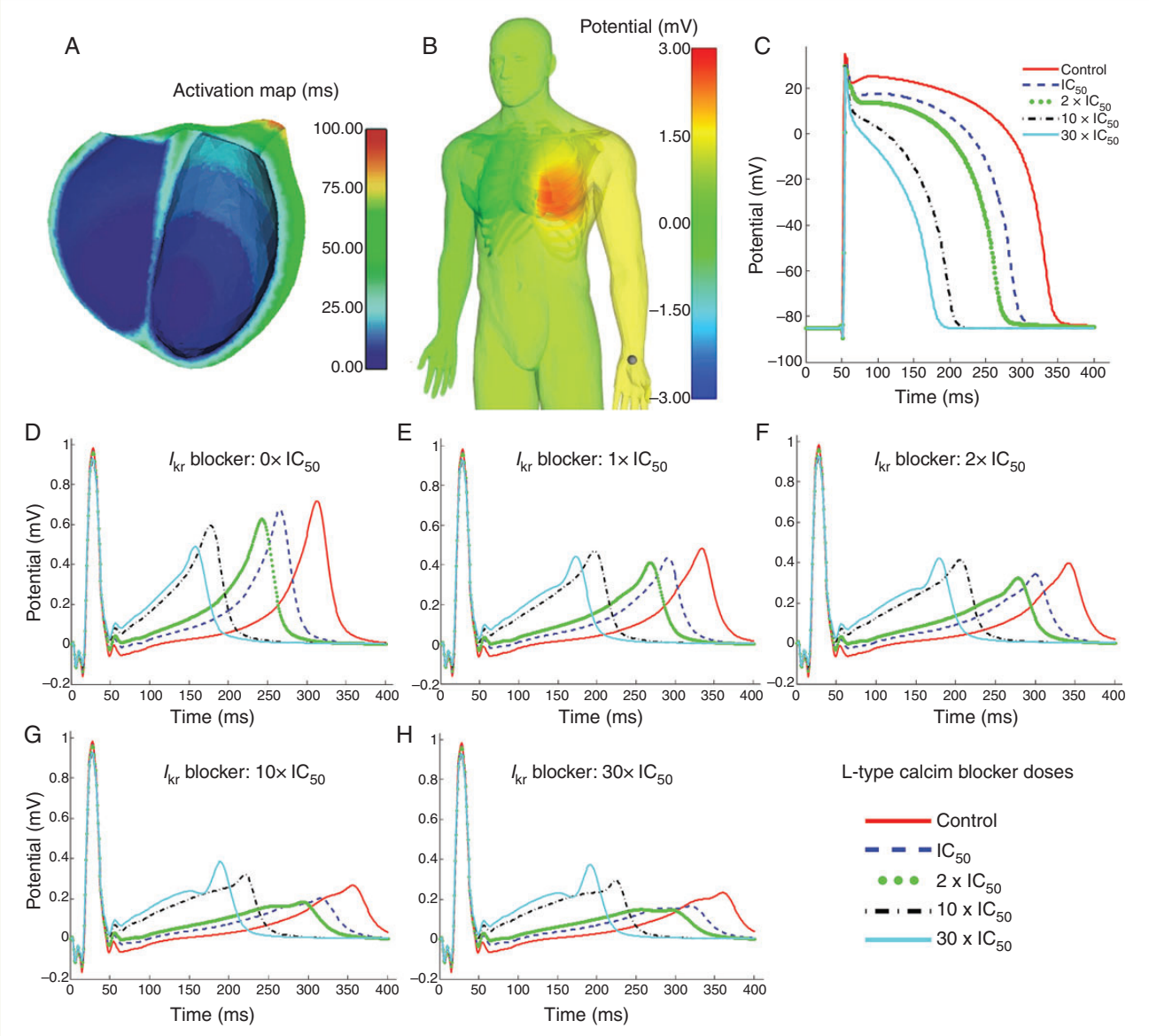

Figure 1 (*A*) A cross-section of the human ventricles showing the activation times map transmurally and on the endocardium. (*B*) Distribution of the body surface potential (right) for the IC_{50} I_{CaL} block dose in a snapshot taken during the repolarization phase. (*C*) Simulated effect of different doses (control, 1× IC_{50}, 2× IC_{50}, 10× IC_{50}, 30× IC_{50}) of I_{CaL} blocker on a representative ventricular AP at a point located at the base of the ventricles. *X*-axis time (ms). *Y*-axis potential (mV). (*D*–*H*) Simulated effect of combined I_{CaL} and I_{Kr} blockers on the second lead of the ECG. Drug dose is 0× IC_{50}, 1× IC_{50}, 2× IC_{50}, 10× IC_{50}, and 30× IC_{50} for I_{Kr} blocker in Panels *D*–*H*, respectively, and in each panel a different dose of I_{CaL} block is shown with a different colour as shown in the legend. *X*-axis shows time in ms, *Y*-axis potential in mV

node located at the base of the left ventricle. Previous studies have linked changes in T-wave amplitude with the Wilson ventricular gradient, which is the gradient of the transmembrane potential in the ventricles.[25,26] As in references,[27–29] we therefore quantified the Wilson ventricular gradient by computing the spatial dispersion of ventricular repolarization. To do so, the spatial dispersion of transmembrane potential throughout the human ventricles is calculated at each time step during the simulations, as the voltage difference between the maximal and minimal values of the transmembrane potential throughout the ventricles at each time step. Its maximum value over time during the repolarization phase is quantified and referred to in the paper as the maximum (spatial) dispersion of transmembrane potential, for each simulation.

Results

The human whole-ventricular model embedded in the torso (*Figure 1A* and *B*) was used to simulate the effect of I_{CaL} and I_{Kr} blocks on ventricular electrophysiology and the ECG. *Figure 1C* shows the simulated effect of I_{CaL} block on the AP for blocker dose [*D*] increasing from zero (control) to [*D*] = IC_{50}, 2× IC_{50}, 10× IC_{50}, and 30× IC_{50} (corresponding to 50, 66, 90, and 96% of

I_{CaL} block, respectively). Increasing I_{CaL} blocker dose results in decrease in AP amplitude and shortening of APD_{90}. Indeed APD_{90} shortens from 290 ms in control to 242, 219, 150, and 126 ms for I_{CaL} block dose of $[D] = IC_{50}, 2\times IC_{50}, 10\times IC_{50}, 30\times IC_{50}$, respectively. The effect of I_{Kr} block was shown in our previous work,[15] and as expected, it leads to a progressive prolongation of the APD_{90} from 290 ms in control conditions to 312 ms for IC_{50} I_{Kr} block, and to 320, 334, and 337 ms) for $2\times$ IC_{50}, $10\times$ IC_{50}, and $30\times$ IC_{50} I_{Kr} block dose, respectively. This corresponds to APD_{90} prolongation by 7.5, 10, 15, and 16% for IC_{50}, $2\times$ IC_{50}, $10\times$ IC_{50}, and $30\times$ IC_{50} I_{Kr} block dose, respectively.

Drugs often exhibit multichannel action and therefore their effects on the heart are difficult to interpret. This is especially the case, when the ion channels affected by the drug have counteracting effects on cardiac behaviour such as I_{CaL} and I_{Kr}, inward and outward currents, respectively, and both important during the plateau and repolarization phases of the human ventricular AP. Therefore, simulations using the human torso model were conducted to investigate the effect of combined I_{CaL} and I_{Kr} blocks on the ECG for 25 different dose combinations. *Figure 1D–H* displays ECG traces obtained for five I_{CaL} block doses, for no I_{Kr} block (e.g. control, *Figure 1D*), and IC_{50}, $2\times$ IC_{50}, $10\times$ IC_{50}, $30\times$ IC_{50} doses of I_{Kr} blocker (*Figure 1E–H*, respectively).

For all I_{Kr} blocker doses, the most notable effects of increasing I_{CaL} block in the ECG are a progressive shortening of the QT interval and simultaneous elevation of the ST segment with increasing dose. Indeed, the QT interval decreases from 315 ms in control to 265 ms (by 15%) for I_{CaL} block dose of IC_{50}, to 240 ms (by 23%) for $2\times$ IC_{50}, to 176 ms (by 44%) for $10\times$ IC_{50} dose, and to 157 ms (by 57%) for I_{CaL} block dose of $30\times$ IC_{50}. The ECG changes caused by I_{CaL} block in *Figure 1D–H*, and specifically the QT shortening, are explained by the AP changes shown in *Figure 1C*, and in particular the decrease in both APD and plateau levels caused by the reduced I_{CaL} as blocker dose is increased. Our simulation results also show that when I_{Kr} block is added to I_{CaL} block, QT shortening still occurs but becomes milder due to the APD_{90} prolongation effects of I_{Kr} block. In addition, increasing I_{Kr} block results in significant decrease in T-wave peak for all I_{CaL} blocker doses, as shown when comparing *Figure 1D–H*.

The simulated effects of combined I_{CaL} and I_{Kr} blocks on the human ECG are further illustrated and examined in *Figure 2*. The second lead of the ECG is shown in *Figure 2A* superimposed for different combinations of IC_{50} and $2\times$ IC_{50} block. As previously shown in *Figure 1*, selective I_{Kr} block prolongs the QT whereas selective I_{CaL} block shortens it, in line with their respective effects on the APD of human ventricular myocytes. In both cases, the T-wave amplitude decreases, in a larger amount for I_{Kr} than for I_{CaL} block (as shown in *Figure 1D–H*). Combined I_{Kr} and I_{CaL} blocks result in more moderate changes in QT than single channel block due to the counteracting effects of the two current blocks on the APD. Furthermore, *Figure 2A* shows that I_{Kr} block does not affect the QRS interval, whereas I_{CaL} block slightly widens it, due to a very small slowing of the conduction velocity.

Figure 2B illustrates the simulated effect of simultaneous I_{CaL} and I_{Kr} block on the distribution of APD_{90} values in a transmural cross-section of the human ventricular model used in the simulations. The panels in *Figure 2B* correspond to increasing I_{CaL} block from top to bottom and to increasing I_{Kr} block from left to right. As expected, the simulations show that overall APD_{90} shortens with increasing I_{CaL} blocker dose, whereas it is prolonged when increasing I_{Kr} block dose. Combined block results in moderate APD_{90} shortening throughout the ventricles, which explains the moderate QT shortening seen in *Figure 2A*. In all cases, the epicardial surface shows shorter APD values than mid-myocardial and endocardial tissue resulting in transmural dispersion in APD_{90}. The APD maps also show how dispersion in APD_{90} is modulated by different degrees of I_{CaL} and I_{Kr} blocks (*Figure 2B*).

Figure 3 shows a quantification of the APD_{90} in a selected node at the base of the ventricles (*Figure 3A*), QT interval (*Figure 3B*), and maximum spatial dispersion of transmembrane potential (*Figure 3C*) for the 25 combined doses of I_{CaL} and I_{Kr} blocks considered in the simulations. *Figure 3A* provides further quantification of the fact that combined I_{CaL} and I_{Kr} blocks at similar doses (diagonal of *Figure 2B*) results in APD_{90} shortening by 23 and 40 ms for IC_{50} and $2\times$ IC_{50} doses for both currents, respectively. Simulation results therefore reflect the fact that APD_{90} using our human model is more sensitive to I_{CaL} block than to I_{Kr} block for a similar drug dose with respect to the IC_{50}. This is also reflected in the QT interval, quantified for the 25 simulations in *Figure 3B*. Therefore, as for APD_{90}, the effect of I_{CaL} block on reducing the QT interval is more pronounced than the prolongation caused by I_{Kr} block for the same degree of block.

As shown in *Figures 1* and *2*, the decrease in the T-wave amplitude is more pronounced for I_{Kr} than for I_{CaL} block. It decreases from 0.72 mV in control to 0.68 and 0.64 mV for IC_{50} and $2\times$ IC_{50} dose of I_{CaL} blocker, whereas it decreases from 0.72 mV to 0.48 and 0.39 mV) for IC_{50} and $2\times$ IC_{50} dose of I_{Kr} blocker. Alterations in the T-wave amplitude in our simulations are complex and affected by heterogeneous changes in AP morphology and duration. Our results show that they could be explained, at least in part, by alterations in the maximum dispersion of transmembrane potential, which result from the changes in heterogeneity in APD_{90} illustrated in *Figure 2B*. As shown in the histograms in *Figure 3C*, both I_{CaL} and I_{Kr} blockers result in maximum spatial dispersion of transmembrane potential below its value in control. The decrease in maximum dispersion caused by I_{Kr} block is more pronounced than the decrease caused by I_{CaL} block for similar doses. This is in line with the decrease in T-wave peak shown in the ECG in *Figure 1D–H*.

Figure 3C also shows that the maximum spatial dispersion of transmembrane potential decreases with increasing I_{CaL} block dose up to $10\times$ IC_{50}. Further increase in I_{CaL} block dose results in a trend inversion: the maximum dispersion of transmembrane potential is higher for $30\times$ IC_{50} than for $10\times$ IC_{50} (but still smaller than in control). This could be explained by the fact that for $30\times$ IC_{50} I_{CaL} block dose, the AP repolarization phase becomes very sharp, as illustrated in *Figure 1C*. Sharp repolarization phases of the AP result in large spatial gradients in transmembrane potential throughout the human ventricles. As shown in *Figure 1E–H*, the increased transmembrane potential gradient also results in higher values of the T-wave peak in the ECG, for $30\times$ IC_{50} than for $10\times$ IC_{50} I_{CaL} block dose.

Discussion

In this work, we have shown the ability of computer simulations to provide insights into the effect of multiaction ion channel blockers on the electrical activity of the human heart and its reflection on

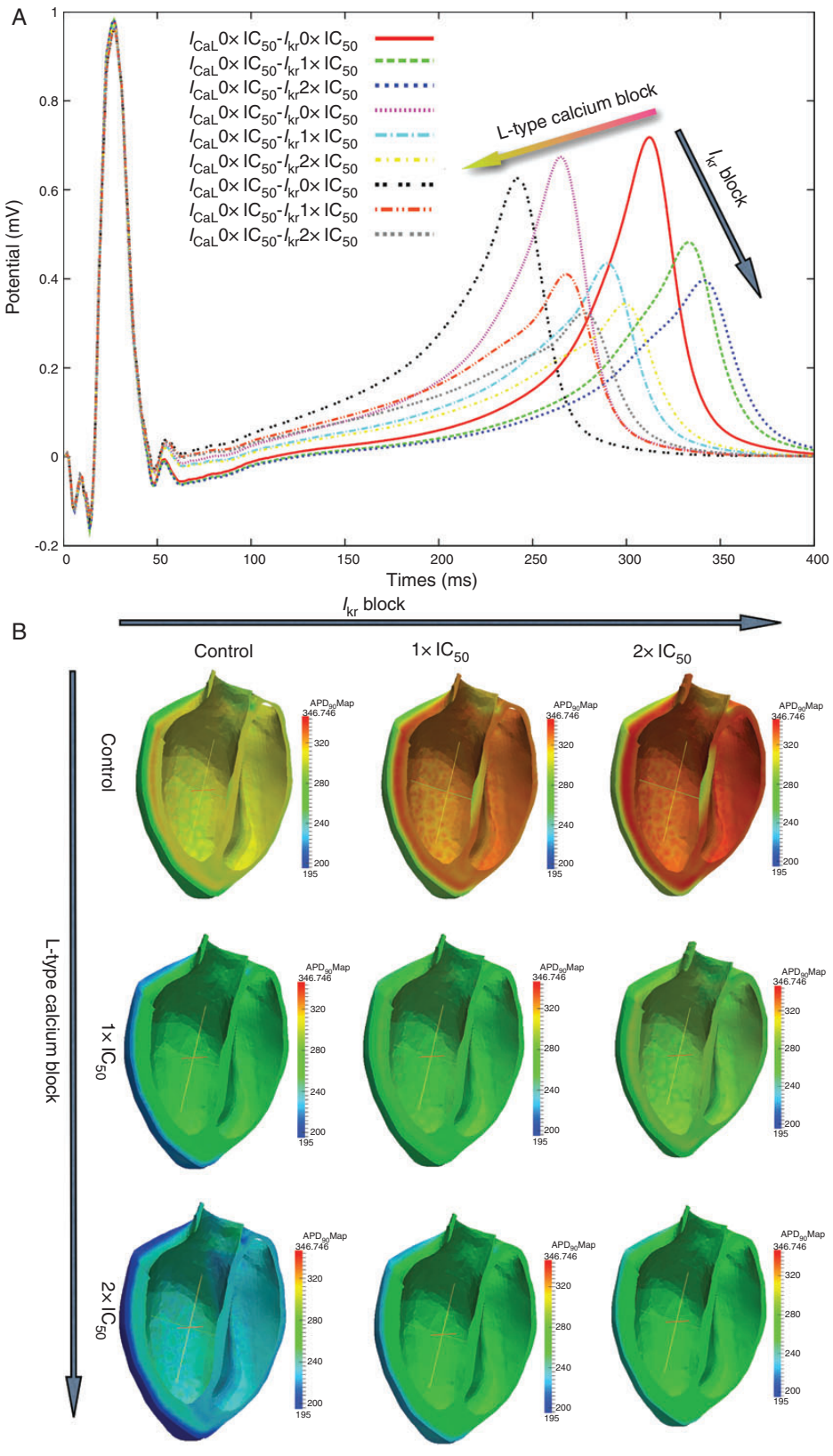

Figure 2 (*A*) Effect of different combinations of I_{Kr} and I_{CaL} blocks doses (0× IC_{50}, 1× IC_{50}, 2× IC_{50}) on the second lead of the ECG. *X*-axis time (ms). *Y*-axis potential (mV). (*B*) Effect of different combinations of I_{Kr} (0× IC_{50}, 1× IC_{50}, 2× IC_{50}) from left to right and I_{CaL} (0× IC_{50}, 1× IC_{50}, 2× IC_{50}) from top to bottom on the APD_{90} distribution. Colour bar in millisecond.

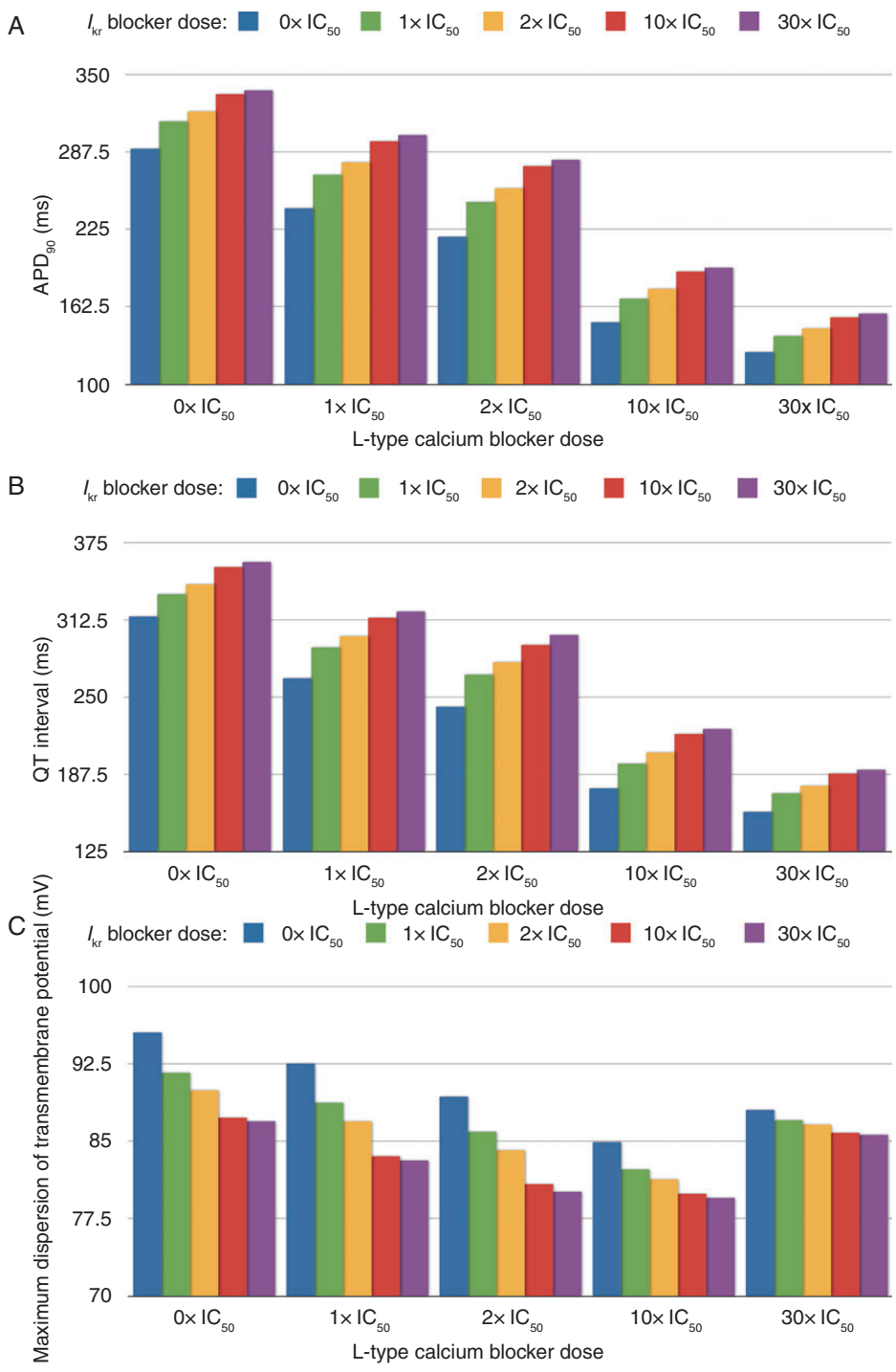

Figure 3 Effect of combining doses of L-type calcium and hERG blockers (control, 1× IC_{50}, 2× IC_{50}, 10× IC_{50}, 30× IC_{50}) on the QT interval (units are mV, ms, and ms, respectively) (*A*), on the APD_{90} (*B*), and on the maximum dispersion of the transmembrane potential during the repolarization phase (*C*). The APD_{90} is computed from a point located at the base of the left ventricle.

the body surface ECG. This is possible through the use of a multiscale human torso–heart anatomical model with biophysically detailed representation of human ventricular membrane dynamics, fibre orientation, and electrophysiological heterogeneity. Our study extends our previous work showing the effect of potassium and sodium channel block on the ECG.[15,16] Here, we focus on investigating the manifestation of the simultaneous block of the inward I_{CaL} and the outward I_{Kr} on human whole-ventricular activity, which has opposite effects on cardiac repolarization and therefore presents a challenge in the interpretation of the ECGs.

Our results show that I_{CaL} block results in shortening of the QT interval, reduction of T-wave amplitude, elevation of the ST segment, and slight widening of the QRS complex. The changes in the ECG are explained by the shortening of APD, reduction of AP amplitude during the plateau phase, decrease of maximum dispersion of the transmembrane potential, and a slight reduction in conduction velocity.

Clinical data on the effect of calcium blockers on the ECG have mostly focused on their effect on the atria and the atrioventricular node,[30,31] rather than in the human ventricles and the ECG, and often in combination with other drugs. Our simulation results are however in agreement with experimental studies reporting APD and QT shortening caused by verapamil in feline wedge preparations.[32] Furthermore, the QT interval shortening and the ST segment elevation in human have also been linked to L-type calcium channel function. Thus, Antzelevitch *et al.*[33] reported that gene mutations mainly in CACNA1C and CACNB2 result in loss of I_{CaL} function and cause a QT shortening and ST elevation, as reported in our simulations. It has also been reported in Proano *et al.*[34] that overdoses of calcium blockers come with abnormalities in T-wave and ST segment. These abnormalities could be seen in our simulation in *Figure 1D* and *E* for high doses of L-type calcium block (e.g. $10\times$ IC_{50} and $30\times$ IC_{50}).

Our theoretical investigation aims at providing new insights, which could be valuable for ECG interpretation. The combined action of I_{CaL} and I_{Kr} blocks investigated in our study is particularly interesting as the two currents have opposite effects on cardiac repolarization and therefore lead to complex and counteracting changes in ECG biomarkers with difficult interpretation. Our results show that the main effect of I_{CaL} block on the ECG is QT shortening and slight ST elevation, whereas I_{Kr} block results in QT prolongation and T-wave peak reduction. The simultaneous application of I_{Kr} and I_{CaL} blocks in doses from IC_{50} to $30\times$ IC_{50} block results in overall decrease in APD and QT interval, which means that for a similar IC_{50}/dose relationship, the effect of I_{CaL} block on the APD and QT interval is more pronounced than I_{Kr} block in our human model.

Importantly, our simulations show that I_{Kr} block effects are more important in determining the T-wave amplitude than I_{CaL} block. Moreover for high doses of I_{Kr} block, our study shows that there is a critical dose of I_{CaL} block, in this case $10\times$ IC_{50}, in the regulation of T-wave peak: lower I_{CaL} blocker doses reduce the T-wave amplitude and higher doses, increases the T-wave amplitude. Our results suggest that the maximum spatial dispersion in transmembrane potential during the repolarization phase plays an important role in this modulation, as suggested by results shown in (*Figure 3C*).

A strong correlation is seen between changes in APD and QT interval caused by both I_{Kr} and I_{CaL} blocks and also by their combination. This is mainly due to the fact that both of I_{Kr} and I_{CaL} blockers affect the repolarization phase, and have negligible effects during the depolarization of the AP, as shown in our simulations. Therefore, I_{Kr} and I_{CaL} blockers also have negligible effects on conduction velocity, activation patterns under sinus rhythm and therefore the QRS complex is not affected (*Figures 1* and *2*). The QT interval is therefore mostly affected by changes in APD. In the presence of sodium blockers however, as considered in our previous study,[15] increasing drug dose results in changes in activation sequence and a prolongation of the QRS and QT interval durations, without any significant effects on the APD. Therefore, the QT interval prolongation caused in the presence of sodium block is not solely correlated with APD.

The human torso–heart model presented in our study could be used to simulate additional drug effects, and our results could be of value to guide the evaluation and interpretation of ECG data obtained following application of Class III and Class IV blockers exhibiting multichannel action.[35,36] Future work could also extend our work to include inter-subject variability in anatomy and electrophysiology[37,38] and by extending the simple pore block drug model to more comprehensive models of drug/ion channel interactions, especially when arrhythmic mechanisms are investigated.[11,22,39] Furthermore, the human whole-ventricular model includes transmural heterogeneities in ionic currents but neglects the potential contribution of apex–base and left-to-right heterogeneities.[40,41] The simulation study by Okada *et al.*[19] shows however that the presence of transmural heterogeneities is sufficient to produce ECGs with the right polarity of the T-wave, whereas apex-to-base heterogeneities need to be very large to produce an effect on the ECG. We therefore believe that apex-to-base and left-to-right heterogeneities as measured in the *in vivo* human ventricles are likely to produce a small modulation of the results presented in this study and could be the focus of future investigations.

Conclusion

In this study, we present a simulation study of the effect of ion channel block on the electrical activity of the heart from drug/ion channel interactions to the ECG. The human bidomain model of the heart embedded in a torso allows for ECG simulations to be conducted with realistic representation of human anatomy and electrophysiological function, and could be used for further investigations including specific drug effects or disease conditions. We show how I_{CaL} block reduces the APD and the AP amplitude during the plateau phase, which, in the ECG, results in ST elevation, QT interval shortening, and slight T-wave amplitude reduction. As drugs often exhibit multiple channel effects, we evaluated the simultaneous effect of I_{CaL} and I_{Kr} on human cardiac activity. As expected, I_{CaL} and I_{Kr} blocks have opposite effects on the QT interval of the ECG: I_{CaL} reduces the QT interval whereas I_{Kr} prolongs it. However, QT interval is more sensitivity to I_{CaL} block, and therefore combined block results in QT shortening. On the contrary, T-wave amplitude is mostly determined by I_{Kr} block dose, even though both I_{CaL} and I_{Kr} decrease T-wave peak. Our simulations show that modulation of the T-wave peak in most cases reflects changes in the maximum spatial dispersion of transmembrane potential. Finally, our study illustrates how the multiscale nature of our human torso/heart model allows for the assessment of the consequences of drug-induced ionic changes on the AP at the cell level, on the APD distribution throughout the ventricles, activation and repolarization maps at the organ level, and on the ECG at the body surface level. Both the human model and the insights provided by the simulation study could contribute to a better characterization of drug-induced effects on the heart for pre-clinical drug testing and also to unravel the ionic basis of new biomarkers of predicting drugs cardiotoxicity.

Acknowledgements

The authors thank Drs Philippe Moireau, Miguel Fernandez, and Elsie Phe from INRIA Paris-Rocquencourt for their work on the anatomical models and meshes. We are also grateful to Professors Dominique Chapelle and Jean-Frederic Gerbeau heads of MACS and REO teams, respectively, in INRIA Paris-Rocquencourt for providing us with the meshes.

Conflict of interest: none declared.

Funding

This study was supported financially by the European Commission preDiCT grant (DG-INFSO—224381), a UK Medical Research Council Career Development Award (to B.R.) and a UK Wellcome Trust Senior Fellowship in Basic Biomedical Sciences (to B.R.). Funding to pay the Open Access publication charges for this article was provided by the UK Wellcome Trust Senior Fellowship in Basic Biomedical sciences.

References

1. Hockerman G, Peterson B, Johnson B, Catterall W. Molecular determinants of drug binding and action on l-type calcium channels. *Annu Rev Pharmacol Toxicol* 1997;**37**:361–96.
2. Furberg CD, Psaty BM, Meyer JV. Nifedipine: dose-related increase in mortality in patients with coronary heart disease. *Circulation* 1995;**92**:1326–31.
3. Pahor M, Guralnik JM, Corti MC, Foley DJ, Carbonin P, Havlik RJ. Long-term survival and use of antihypertensive medications in older persons. *J Am Geriatr Soc* 1995;**43**:1191–7.
4. Pahor M, Guralnik JM, Ferruci L, Corti MC, Salive ME, Cerhan JR *et al.* Calcium-channel blockade and incidence of cancer in aged populations. *Lancet* 1996;**348**:493–9.
5. Bodi I, Mikala G, Koch S, Akhter S, Schwartz A. The L-type calcium channel in the heart: the beat goes on. *J Clin Invest* 2005;**115**:3306–17.
6. Davies MR, Mistry HB, Hussein L, Pollard CE, Valentin JP, Swinton J *et al.* An *in silico* canine cardiac midmyocardial action potential duration model as a tool for early drug safety assessment. *Am J Physiol Heart Circ Physiol* 2012;**302**:1466–80.
7. Mirams GR, Cui Y, Sher A, Fink M, Cooper J, Heath BM *et al.* Simulation of multiple ion channel block provides improved early prediction of compounds clinical torsadogenic risk. *Cardiovasc Res* 2011;**91**:53–61.
8. Rodriguez B, Burrage K, Gavaghan D, Grau V, Kohl P, Noble D. The systems biology approach to drug development: application to toxicity assessment of drug toxicity. *Nat Clin Pharmacol Ther* 2010;**88**:130–4.
9. Wilhelms M, Rombach C, Scholz EP, Doessel O, Seemann G. Impact of amiodarone and cisapride on simulated human ventricular electrophysiology and electrocardiograms. *Europace* 2012;**14**:90–6.
10. Carusi A, Burrage K, Rodriguez B. Bridging experiments, models and simulations: an integrative approach to validation in computational cardiac electrophysiology. *Am J Physiol Heart Circ Physiol* 2012;**303**:144–55.
11. Moreno JD, Clancy CE. Using computational modelling to predict arrhythmogenesis and antiarrhythmic therapy. *Drug Discov Today* 2009;**6**:71–84.
12. Quinn TA, Kohl P. Combining wet and dry research: experience with model development for cardiac mechano-electric structure-function studies. *Cardiovasc Res* 2013;**97**:601–11.
13. Trayanova NA. Whole-heart modeling: applications to cardiac electro-physiology and electromechanics. *Circ Res* 2011;**108**:113–28.
14. Corrias A, Jie X, Romero L, Bishop MJ, Bernabeu M, Pueyo E *et al.* Arrhythmic risk biomarkers for the assessment of drug cardiotoxicity: from experiments to computer simulations. *Philos Trans R Soc A, Math Phys Eng Sci* 2010;**368**:3001–25.
15. Zemzemi N, Bernabeu M, Saiz J, Cooper J, Pathmanathan P, Mirams GR *et al.* Computational assessment of drug-induced effects on the electrocardiogram: from ion channel to body surface potentials. *Br J Pharmacol* 2013;**168**:718–33.
16. Zemzemi N, Bernabeu MO, Saiz J, Rodriguez B. Simulating drug-induced effects on the heart: from ion channel to body surface electrocardiogram. Functional Imaging and Modeling of the Heart 2011;0:259–66.
17. Chapelle D, Fernndez MA, Gerbeau JF, Moireau P, Sainte-Marie J, Zemzemi N. Numerical simulation of the electromechanical activity of the heart. Functional Imaging and Modeling of the Heart, volume 5528 of Lecture Notes in Computer Science 2009;357–65.
18. Ten Tusscher K, Panfilov AV. Cell model for efficient simulation of wave propagation in human ventricular tissue under normal and pathological conditions. *Phys. Med Biol* 2006;**51**:6141–56.
19. Okada JI, Washio T, Maehara A, Momomura SI, Sugiura S, Hisada T. Transmural and apicobasal gradients in repolarization contribute to T-wave genesis in human surface ECG. *Am J Physiol Heart Circ Physiol* 2011;**301**:200–8.
20. Zemzemi N. Etude theorique et numerique de l'activite electrique du Coeur: Application aux electrocardiogrammes. *DPhil Thesis*. 2009. http://tel.archives-ouvertes.fr/tel-00470375/en/
21. Durrer D, van Dam RT, Freud GE, Janse MJ, Meijler FL, Arzbaecher RC. Total excitation of the isolated human heart. *Circulation* 1970;**41**:899–912.
22. Brennan T, Fink M, Rodriguez B. Multiscale modelling of drug-induced effects on cardiac electrophysiological activity. *Eur J Pharm Sci* 2009;**36**:62–77.
23. Mirams GR, Arthurs CJ, Bernabeu MO, Bordas R, Cooper J, Corrias A *et al.* Chaste: an open source C++ library for computational physiology and biology. *PLoS Comput Biol* 2013;**9**:970–1002.
24. Pitt-Francis J, Pathmanathan P, Bernabeu MO, Bordas R, Cooper J, Fletcher AG *et al.* Chaste: a test-driven approach to software development for biological modelling. *Comput Phys Commun* 2009;**180**:2452–71.
25. Draisma HH, Schalij MJ, van der Wall EE, Swenne CA. Elucidation of the spatial ventricular gradient and its link with dispersion of repolarisation. *Heart Rhythm* 2006;**3**:1092–9.
26. Plonsey R. A Contemporary view of the ventricular gradient of Wilson. *J Electrocardiol* 1979;**12**:337–41.
27. Antzelevitch C. Transmural dispersion of repolarisation and the T wave. *Cardiovasc Res* 2001;**50**:426–31.
28. Behrens S, Li C, Knollmann BC, Michael RF. Dispersion of ventricular repolarisation in the voltage domain. *Pacing Clin Electrophysiol* 1998;**21**:100–7.
29. Yan GX, Antzelevitch C. Long-QT syndrome cellular basis for the normal T wave and the electrocardiographic manifestations of the long-QT syndrome. *Circulation* 1998;**98**:1928–36.
30. Somogyi A, Albrecht M, Kliems G, Schafer K, Eichelbaum M. Pharmacokinetics, bioavailability and ECG response of verapamil in patients with liver cirrhosis. *Br J Clin Pharmacol* 1981;**12**:51–60.
31. Wood MA, Gilligan DM, Brown-Mahoney C, Nematzadeh F, Stambler BS, Ellenbogen KA. Clinical and electrophysiologic effects of calcium channel blockers in patients receiving ibutilide. *Am Heart J* 2002;**143**:176–80.
32. Aiba T, Shimizu W, Inagaki M, Noda T, Miyoshi S, Wei-Guang D *et al.* Cellular and ionic mechanism for drug-induced long QT syndrome and effectiveness of verapamil. *J. Am Coll Cardiol* 2005;**45**:300–7.
33. Antzelevitch C, Pollevick GD, Cordeiro JM, Casis O, Sanguinetti MC, Aizawa Y *et al.* Loss-of-function mutations in the cardiac calcium channel underlie a new clinical entity characterized by ST-segment elevation, short QT intervals, and sudden cardiac death. *Circulation* 2007;**115**:442–9.
34. Proano L, Chiang WK, Wang RY. Calcium channel blocker overdose. *Am J Emerg Med* 1995;**13**:444–50.
35. Huang ZJ, Dai DZ, Li N, Na T, Ji M, Dai Y. Calcium antagonist property of CPU228, a dofetilide derivative, contributes to its low incidence of torsades de pointes in rabbits. *Clin Exp Pharmacol Physiol* 2007;**34**:310–7.
36. Prystowsky EN. Effects of bepridil on cardiac electrophysiologic properties. *Am J Cardiol* 1992;**69**:63D–7D.
37. Britton O, Bueno-Orovio A, Van Ammel K, Lu HR, Towart R, Gallacher D *et al.* Experimentally-calibrated population of models predicts and explains inter-subject variability in cardiac cellular electrophysiology. *Proc. Natl Acad Sci USA* 2013;**110**:2098–105.
38. Walmsley J, Rodriguez JF, Mirams GR, Burrage K, Efimov IR, Rodriguez B. mRNA expression levels in failing human hearts predict cellular electrophysiological remodelling: a population-based simulation study. *PLoS ONE* 2013;**8**:e56359.
39. Moreno JD, Clancy CE. Pathophysiology of the cardiac late Na current and its potential as a drug target. *J Mol Cell Cardiol* 2012;**52**:608–19.
40. Bueno-Orovio A, Hanson B, Gill J, Taggart P, Rodriguez B. *In vivo* human left-to-right ventricular differences in rate adaptation transiently increase pro-arrhythmic risk following rate acceleration. *PLoS ONE* 2012;**7**:e52234.
41. Ramanathan C, Jia P, Ganem R, Ryu K, Rudy Y. Activation and repolarization of the normal heart under complete physiological conditions. *Proc Natl Acad Sci USA* 2006;**103**:6309–14.